Available online at www.sciencedirect.com

ScienceDirect

Procedia CIRP 59 (2017) 144 – 149

www.elsevier.com/locate/procedia

The 5th International Conference on Through-life Engineering Services (TESConf 2016)

The combination of advanced tools for parameters investigation and tools maintenance in flow forming process

A. D'Annibale[a*], A. Di Ilio[b], A. Paoletti[c], D. Paoletti[d]; S. Sfarra[e]

[a,b,c,d,e] *Dept of industrial and Information Engineering and Economics, Universityof l'Aquila, Via G. Gronchi, 18, 67100, L'Aquila, Italy*

* Antonello D'Annibale. *E-mail address:* antonello.dannibale@univaq.it

Abstract

In this work, the authors present an investigation on technological parameters affecting the flow forming process of aluminum alloy 6060 tubular structures and to discuss about the tools maintenance. Flow forming tests were carried out by mounting a single roller on a lathe machine. A 3D thermo-mechanical finite element model was developed to analyze the interaction between the roller and the workpiece in terms of forces, strains and thermal distribution. The effects of friction conditions were investigated through the FE model results and comparing them with acquired thermal maps. The model was validated by comparing the geometrical characteristics of the workpieces, such as the axial elongation, the inner and outer tube diameter. Aluminum spring-back was taken into account with material model adopted in the numerical algorithm. Once collected a complete information on the process parameters, some thermal images were acquired on roller in order to find a parameters set able to reduce the stresses acting on it as far as to obtain the maximum elongation with the minimum number of passes.

Peer-review under responsibility of the scientific committee of the The 5th International Conference on Through-life Engineering Services (TESConf 2016)

Keywords: thermal analysis, Finite Element Analysis, flow forming, tools maintenance.

1. Introduction

Flow forming technology finds application in manufacturing of high performance components, often in conjunction with the need to reduce the number of different parts which form an assembly. In particular, it can be used for selective thinning of hollow cylindrical components with the goal to product structures with uniform resistance for lightweight parts, which have a great demand in the automotive industry. Flow forming is considered as the most advanced technology due to the advances reached in comparison with other techniques as extrusion and tube drawing. In particular, several researchers were investigating on high strength and high precision rotational symmetry achieved with this kind of process, moreover on surface finish as well as the flexibility to be used with different tubular sections and materials.

Sivanandini et al. [1] described many interesting aspects of flow formability focusing on a 3 roller flow forming operation, involving a cylindrical tube and illustrated the possibility to form axisymmetric parts with complex sections, as possible answer especially to automotive industry demand. Xia et al. [2] focused on many different possibilities given by flow forming, investigating on process parameters in non-asymmetrical, non-circular cross section and tooth shaped spinning. Differently from [1], [2] referred about the advancement of novel, with particular reference to equipment, presenting a classification method for metal spinning process. This kind of process were classified taking into account material characteristics, roller-blank relative positioning, spindle or spindle free spinning and process temperature.

On process parameters investigations, Chang et al. [3] contributed by investigating experimentally the maximum thickness reduction before fracture (this parameter was called spinnability) on AA2024 and 7075 aluminum alloys. Moreover, Hamid et al. [4] discussed experimentally on the effects of spinning accuracy, surface roughness, percentage of elongation, yield strength and the ultimate strength as a function of thickness reduction. About the study of process

Peer-review under responsibility of the scientific committee of the The 5th International Conference on Through-life Engineering Services (TESConf 2016)
doi:10.1016/j.procir.2016.09.038

parameters effects studied with experiments, Davidson et al. [5] focused on spindle speed, cut depth, final diameter and feed rate and their effects respect to the final elongation. Xu et al. [6] used a 3D model based on finite element method to research on diameter variations, waves on cylindrical surface and the reflection of generatrices. Xu et al. used a rigid-plastic material model while Hua et al. [7] by creating a 3D elasto-plastic model investigated on 3 roller backward spinning on a cylindrical sample to study on bell-mouth, build-up, bulging in front of and between rollers and diameter variations.

On the influence of process parameters on microstructure Jahazi et al. [8] focused on the effects of the pre-heat temperature, the holding time and the cooling rate while Chao et al. [9] discussed on characteristics of the microstructure resulting by hot flow forming for thin walled AZ80 magnesium alloys. Besides, Wong et al. [10] researched on roller path and geometry to product a small cup and a boss at the end of the workpiece, while Parsa et al. [11] studied the variations of area to elongation ratios with feed rate and with different attack angles. In term of stresses and strains resulted by different parameters values Naksoo et al. [12] contributed by evaluating the minimum axial force to obtain the optimal attack angle of the roller.

Mohebbi and Akbarzadeh [13] investigated on flow forming parameters with a combination of experiments and numerical models meanwhile the authors in this work focused their attention on a single roller flow forming process. Known the effects of axial and radial feed rate and angular speed by numerical model and verified results with experimental tests on Al 6060 aluminum alloys, the authors investigated on temperature distribution acquiring thermal maps under running process. With thermal distribution on roller and workpiece, the authors were able to discuss on temperature affecting process parameters moreover to preliminary discuss equipment maintenance, with a special attention to roller.

2. Analysis and Finite element modeling

A 3D thermo-mechanical model based on a commercial finite element code (Pam Stamp®) was created to investigate process parameters effects on final tube dimensions. In particular, five different thickness reduction value (i.e. 0.2, 0.4, 0.6, 0.8 and 1.0 mm) were tested with two axial feed rates (0.4 and 0.6 mm/rev), as listed in Table 1. The initial workpiece thickness was 2 mm. Rotational speed was set at 92 rpm for the workpiece therefore assuming no-slip contact conditions, the roller rotational speed is about the half, as indicated by workpiece-roller diameter ratio. As observed in experimental tests, thickness reduction, is listed in column "Pass depth" of Table 1, as also the complete set of parameters taken into consideration in this study. The parameters set and the corresponding results for axial feed rate 0.6 mm/rev are indicated in red colour in Table 1 and in all subsequent tables, while the results obtained a 0.4 mm/rev are reported in black colour.

Table 1 – Process parameters studied with simulations.

Axial feed rate		Rotational speed	Dinitial inner	Dinitial outer	L initial	Pass depth (diametral)
[mm]		[rpm]	[mm]	[mm]	[mm]	[mm]
						0.2
						0.4
0.4	**0.6**	92	48	50.2	110.2	0.6
						0.8
						1

In this study, the roller axis has been assumed parallel to the tube axis. Roller geometry as well as the process parameters taken into consideration in this study are illustrated in Fig. 1. In particular, the roller profile presented a very low angle in the elongation direction in order to distribute plasticized material and to further tube stretching whereas the roller has a very large curvature angle for the opposite side to reduce friction effects. Friction coefficient was set to 0,6 as reported in literature between steel (roller) and aluminum (specimen) and with lubricant conditions (mineral oil in this case) 0,12 was considered.

The specimen was discretized in by about 50,000 tetrahedron elements with closer dimensions in the contact area between workpiece and roller. This fitted region moved with the roller in the elongation direction to detail stresses and strains in the deformation area. The material model was considered elasto-plastic to take into consideration springback effects, which are significant with processes involving aluminum parts. To benefit of a short calculation time and to avoid contact problems during transient, the roller is initially positioned externally from the workpiece with the thickness reduction value already set. Differently, in the experimental tests, the roller is initially moved radially to set the desired thickness reduction and then it is axially moved to obtain stretching. As depicted in Fig. 1, this hypothesis permits to work with the same material volume between experimental and numerical tests but the mesh element number is reduced. In conclusion, with respect to workpiece axial free side, the specimen initial length is considered of 30 mm.

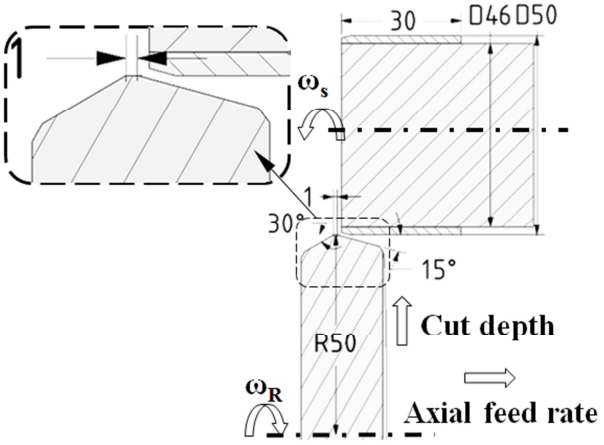

Fig. 1. (a) Tools and sample dimensions with process parameters studied (units in mm); (b) mesh of the initial workpiece.

In the first simulations series the effects of axial feed rate on elongation were analyzed and geometrical results were compared with experimental ones. A second simulations series was conducted to observe the effects of axial feed rate on roller and workpiece thermal distributions. The constitutive law of the material used in the FE model is described by Eq.1:

$$\sigma[\mathrm{MPa}] = 88.7 \cdot \bar{\varepsilon}^{0.62} \cdot \dot{\bar{\varepsilon}}^{0.007} + 68.3 \quad (1)$$

3. Experimental tests

Experimental tests were conducted by mounting a single roller on a lathe. The roller was designed with dimensions shown previously in Fig.1 and constructed with Fe510. This tool is depicted in Fig. 2a. Two experimental series were conducted. In the first one, two different axial feed rates, indicated in Table 1, were tested and measurements were acquired in particular diameter and elongation. The second experimental series was conducted for a feed rate of 0.6 mm/rev in order to detect thermal distribution by a thermal camera and to compare with 0.4 mm/rev results. Three repetitions for each experimental series were carried out and results reported in this paper represent an average of the collected values.

Initially and at the end of the operations, specimen circularity and roundness were checked by means a comparator as depicted in Fig. 2b. Axial elongation and outer diameter of the tube were measured by a caliber in order to compare the results with those obtained from FEM results.

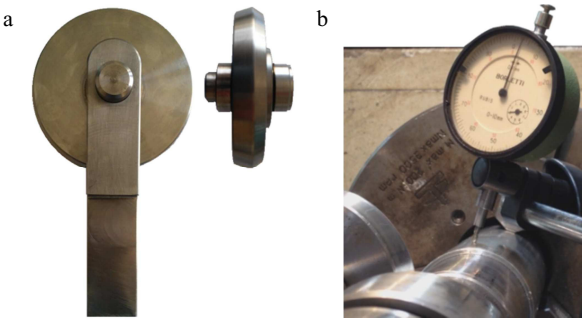

Fig. 2. (a) Roller constructed for the experiments; (b) axial and circumferential variations measured by a comparator.

A plan view of flow forming operation, captured during the running process, is illustrated in Fig. 3a. Mineral oil was used as lubricant and so the emissivity value for thermography was set to 0.95 as suggested in [14]. Dry conditions were not investigated in this study because of the emissivity value of 0.1 could cause higher uncertainty on thermography measurements. As focused on Fig. 3b, the lubricant film is distributed along all the specimen and roller surfaces. Material flow is also visible in Fig. 3b as a deviation of the tube from the cylindrical shape.

The specimens are mounted on a circular bar with a 0.1 mm of clearance and lubricant was added to favour axial stretching. Tube and mandrel were mounted on a self-centering spindle while the roller axis was positioned in parallel to that of the specimen. The assembly was completed by a tailstock to guarantee the axial positioning of the parts and to reduce bending of workpiece and lathe components.

The system was completely shielded with polystyrene walls to avoid environmental and lathe motor radiations.

Relative humidity and environmental temperature were measured and subtracted to the results acquired by the thermal camera. For thermal measurements, ThermaCAM S65 HS by FLIR was employed and 50 Hz was the acquisition frequency.

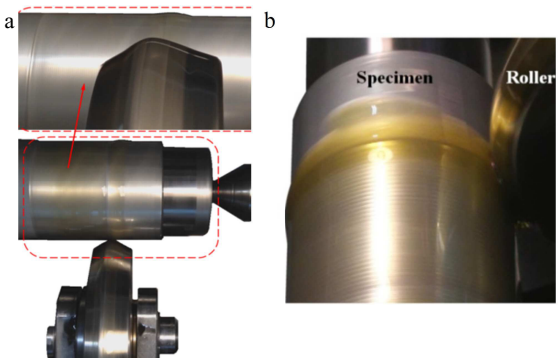

Fig. 3. (a) Plan view of a flow forming operation; (b) lubricant conditions on specimen during running operation.

4. Results

Table 2 shows the results obtained in the two experimental series, where in black and red color the results for axial feed rates 0.4 and 0.6 mm/rev are listed, respectively. With an higher axial feed rate the material flow is larger and final elongation is then different from 0.4 mm. The thickness values reported in Table 2 have been calculated by considering the volume conservation, acquired the elongation values.

Table 2 – Elongations and thickness resulted by experimental tests.

Axial feed rate		Pass depth (diametral)	Lavg		Davg external		Calculated thickness	
[mm]		[mm]	[mm]		[mm]		[mm]	
0.4	**0.6**	0.2	111.0	**111.1**	50.18	**50.18**	2.18	**2.18**
		0.4	111.9	**113.7**	50.17	**50.13**	2.17	**2.13**
		0.6	113.4	**118.4**	50.14	**50.05**	2.14	**2.05**
		0.8	115.1	**122.3**	50.11	**49.99**	2.11	**1.99**
		1	117.0	**130.6**	50.07	**49.86**	2.07	**1.86**

As regards the temperature detection, it must be remarked that the thermal camera was not positioned perpendicularly to the assembly plan view, due to the presence of the protective screen of the spindle. Therefore, such condition could have affected the absolute value of the measurements, which however preserve their significance at the comparative level. In Fig. 4, the temperature distributions after tests with different feed rates are shown. In both the pics in Fig. 4, the roller was kept in the middle of its axial stroke. As can be seen, the temperature profile is quite low, exhibiting a maximum value at the roller contact area, as expected, for both the tests. At 0.6 mm/rev axial feed rate, the average value is about 2 °C higher than the corresponding value at 0.4 mm/rev.

It is possible to observe that the roller exhibits a cold zone in the central fillet radius and a hotter zone on the surface

opposed to material flow. Moreover, the effects of friction on lateral surfaces are highlighted, due to the sliding between roller and brass ring, whose effects will be depicted with thermal images in the discussion. Thermal effects on the mandrel are evidenced only in the zone nearby to the tube stretching side.

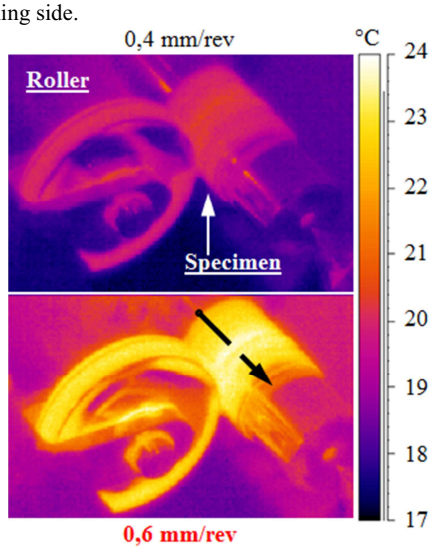

Fig. 4. Thermal image of the running process.

Fig. 5 shows the temperature distribution obtained with the FEM model, in the middle axial stroke of the roller. In the simulation results, the temperature reached in the contact zone is about 2 °C higher than in the other parts. Therefore, the average temperature value is comparable with the experimental results.

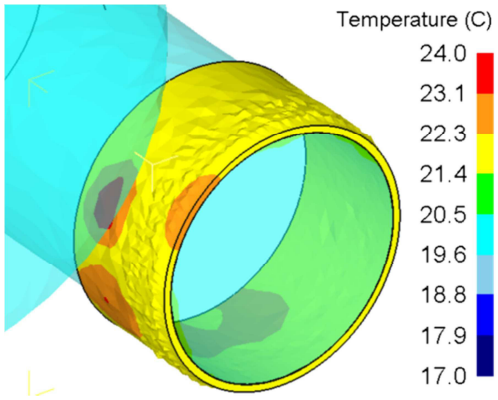

Fig. 5. Temperature distribution resulted by FE model.

5. Discussion

By analyzing the temperature trends for different feed rate values with the other parameters set fixed, the effects on stretching are shown in Fig. 6. At the end of the experimental tests, the cumulative difference ction obtained with the higher feed rate is more pronounced than the one obtained with 0.4 mm/ver. With the higher feed rate, an higher elongation with less passes is obtained. Moreover, temperature effects are similar, with a difference of about 2 °C on temperature distribution.

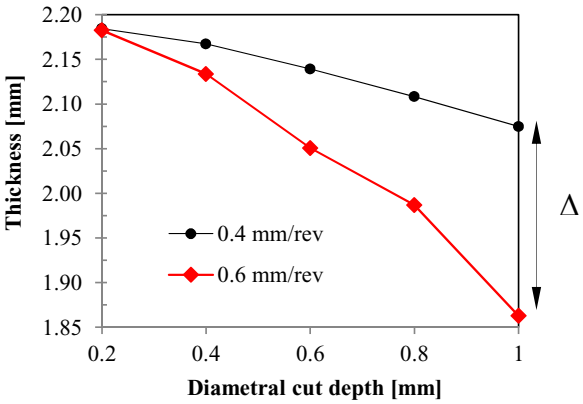

Fig. 6. Thickness trend during different cut depth for two axial feed rates.

A photograph of the specimens obtained in the experimental tests is reported in Fig. 7, where the different axial elongation is highlighted. It can be seen, that the surface finish of the sample obtained at higher feed rate is better and the surface is smoother meanwhile with feed rate 0.4 mm the grooves are larger.

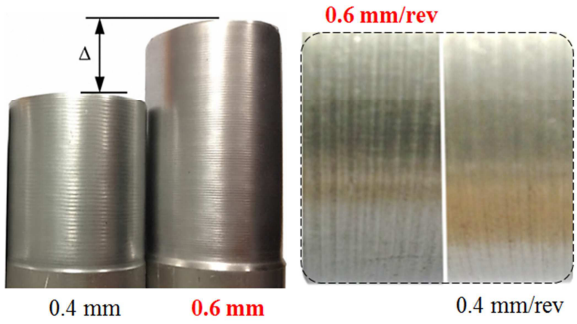

Fig. 7. Specimens resulted with elongation difference (Δ) highlighted.

The surface temperature trend along a workpiece generatrix, highlighted in Fig. 4, allows to characterize the thermal evolution during the process. The temperature profiles deduced from the experimental thermal maps are plotted in Fig. 8 for both feed rates. The diagrams evidence the presence of three zones. The first one, which relates to the already deformed part of the workpiece, exhibits an average value higher with respect to the non-deformed zone (right part of the diagram). The zone under deformation shows thermal spikes which are significantly different for the two cases under examination, being higher at the more elevated feed rate. Despite the peaks are evident, the temperature increase is only about 2 and 4 °C respectively. However it should be remarked that the reported thermal profiles refer to the conditions of the workpiece one revolution after the

deformation has occurred.

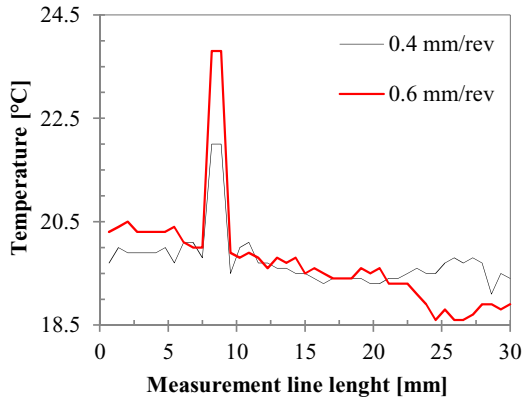

Fig. 8. Temperature trend along the measurement line (experimental result).

Radial force-stroke trend during the whole process was investigated to deepen the effects of temperature distribution. In Fig. 10, radial force is shown with an axial feed rate of 0.6 mm/rev. The effects of the first thickness reduction (0.2 mm measured on diameter) is quite low, while higher radial forces exerted by roller are higher. The shown trend is similar in the different passes: after an increasing portion the forces reach a maximum level and decrease getting out the total length. In the first two passes, force stroke trend presented a curvature after the stationary level, meanwhile this trend disappears in the following passes. This condition is due to the sample length which is smaller in the initial operation while after the second ones the stretching became significant. Acquired information on forces exerted by tool, significant consideration can be discussed about tool maintenance.

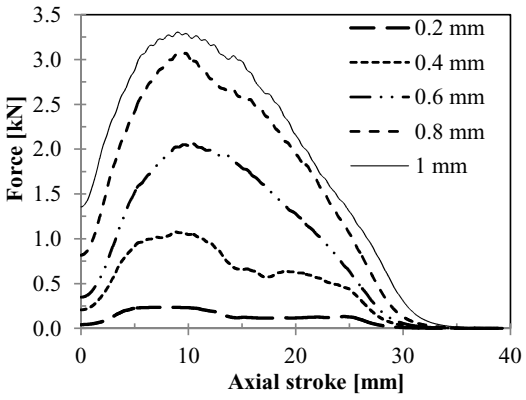

Fig. 9. Force-stroke trend during the whole process of 0,6 mm.

Temperature and Von Mises stress on roller for 0.6 mm/rev feed rate test are shown in Fig. 10 for normal roller condition, i.e. not worn yet. The maximum temperature experienced during the process is about 24 °C and the maximum stress value reached on roller-workpiece contact area is about 100 MPa. Moreover, this value is experienced in particular at the central roller area, which is the one devoted to produce deformation on workpiece. This value is due to mechanical and thermal conditions and this is significant to predict tool life.

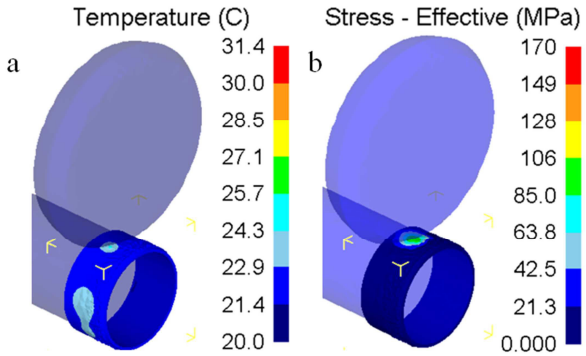

Fig. 10. Results on workpiece at the end of 0,6 mm feed rate process for roller without waste; (a) temperature distribution; (b) effective stress.

The effect of roller wear due to thermal and mechanical conditions was analyzed by the FE model considering a contact surface of 1.5 mm long instead of 1 mm (which represents normal roller conditions) due to wear of the surface caused by boundary conditions. As described by Fig. 11a, temperature distribution on contact area increased significantly of about 7 °C with significant variation of the Von Mises stress, as depicted in Fig. 11b. Moreover, the final sample length is 1.2 mm less than expected. The off-design conditions analyzed should not occur not only for increasing tool life but also to obtain the correct elongation.

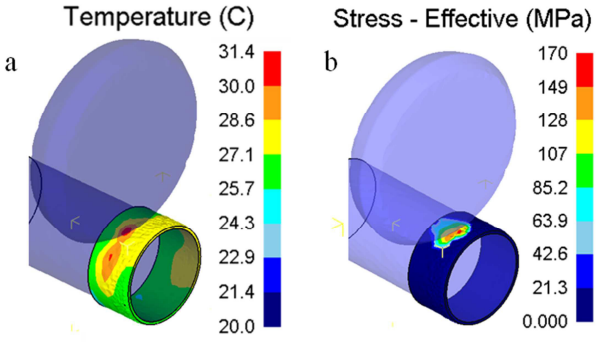

Fig. 11. Results on workpiece at the end of 0,6 mm feed rate process for worn out roller (a) temperature distribution; (b) effective stress.

6. Conclusion

The authors investigated on process parameters effects affecting flow forming process. In particular the effects of feed rate were analyzed on final sample dimensions. To predict process parameters effects a 3D thermo-mechanical FE model based on a commercial code was developed. Two different experimental tests series were carried and thermal maps were acquired on running process. Two feed rate values

were tested and experimental results were compared with FEM results in order to validate the model. Process parameters effects on temperature distribution were investigated. Identified temperature distribution on tools, stressed zone were highlighted and forces exerted for deformation were calculated. For higher feed rates, temperature distribution difference respect to the lower feed rate case was only 2 °C, therefore the elongation difference was significant. Thermal maps in communion with FE algorithm results suggested data input for tool maintenance, permitting consideration on tool life.

Acknowledgements

The authors are grateful to the technicians Giovanni Pasqualoni and Cesare Michetti for their valuable contribution given in carrying out the experimental tests.

References

[1] Sivanandini M, Dhami SS, Flow-Forming of tubes-A Review, International Journal of Scientific & Engineering Research, 2012, Volume 3.
[2] Qinxiang Xia, Gangfeng Xiao, Hui Long, Xiuquan Cheng, Xiangfei Sheng, A review of process advancement of novel metal spinning, International Journal of Machine Tools & Manufacture, 2014, Volume 85, pp. 100–121.
[3] Chang CH, Huang CA, Tube Spinnability of AA2024 and 7075 Alluminium Alloys, Journal Of Materials Processing Technology, 1998, pp. 676–682.
[4] Hamid RM, Faramarz D, Experimental study of thickness reduction effects on mechanical properties and spinning accuracy of aluminum 7075-O, during Flow-Forming, International Journal of Advanced Manufacturing Technology, 2011, Volume 52, pp. 949–957.
[5] Davidson MJ, Balasubramanian K, Experimental Investigation on Flow-Forming of AA6061 Alloy- Taguchi Approach, Journal Of Materials Processing Technology, 2008, pp. 283-287.
[6] Xu Y, Zhang SH, 3-D Rigid-Plastic FEM Numerical Simulation on Tube Spinning, Journal Of Materials Processing Technology, 2001, pp. 710-713.
[7] Hua FA, Yang YS, Zhang YN, Guo MH, Guo DY, Three-dimensional finite element analysis of tube spinning, Tong WH, Hu ZQ, Journal of Materials Processing Technology, Volume 168, 2005, pp. 68–74.
[8] Jahazi M, Ebrahimi G, The Influence of Flow-Forming Parameters and microstructure on the Quality of a D6AC Steel, Journal Of Materials Processing Technology, 2000, Volume 103, pp.362-366.
[9] Chao Z, Wang F, Wan Q, Zhang J, Dong J, Microstructure and mechanical properties of AZ80 magnesium alloy tube fabricated by hot flow forming, Materials and Design, Volume 67, 2015, pp. 64-71.
[10] Wong CC, Lin J, Dean TA, Effects of roller path and geometry on the flow forming of solid cylindrical components, Journal of Materials Processing Technology, Volume 167, 2005 pp. 344–353.
[11] Parsa MH, Pazooki AMA, Ahmadabadi MN, Flow-forming and flow formability simulation, International Journal of Advanced Manufacturing Technology, Volume 42, 2009, pp. 463–473.
[12] Naksoo Kim, Honglae Kim, Kai Jin, Minimizing the Axial Force and the Material Build-up in the Tube Flow Forming Process, International Journal of precision engineering and manufacturing, 2013, Vol. 14, No. 2, pp. 259-266.
[13] Mohebbi MS, Akbarzadeh A, Experimental study and FEM analysis of redundant strains in Flow-Forming of tubes, Journal Of Materials Processing Technology, Volume 210, 2010, pp. 389–395.
[14] http://optotherm.com/emiss-table.htm, April 2016.